High-Temperature Expansions for the Classical Heisenberg Model. I. Spin Correlation Function*

H. EUGENE STANLEY

Lyman Laboratory of Physics, Harvard University, Cambridge, Massachusetts

and

Lincoln Laboratory,† Massachusetts Institute of Technology, Lexington, Massachusetts

(Received 31 January 1967)

The diagrammatic representation of the first nine coefficients for loose-packed lattices and the first eight coefficients for close-packed lattices in a high-temperature series expansion of the zero-field spin correlation function $\langle \mathbf{S}_f \cdot \mathbf{S}_g \rangle_\beta$ is presented. This calculation exploits the order-of-magnitude simplifications which occur in treating the quantum-mechanical spin operators in the Heisenberg model as isotropically interacting classical vectors of length $[S(S+1)]^{1/2}$. This semiclassical approximation—the "classical" Heisenberg model—appears to be excellent for some critical properties of interest if $S > \frac{1}{2}$. A recursion relation is seen to obviate the need to consider the sizeable classes of disconnected diagrams and diagrams containing articulation points. The utility of the high-temperature series for $\langle \mathbf{S}_f \cdot \mathbf{S}_g \rangle_\beta$ is discussed. It contains information which is relevant to current experiments and is not contained in the high-temperature expansions for the thermodynamic functions (e.g., susceptibility, specific heat), as well as providing an efficient method of extending the series for all the thermodynamic functions together. As an example of the applicability of the series expansion of $\langle \mathbf{S}_f \cdot \mathbf{S}_g \rangle_\beta$ to obtain information concerning the short-range magnetic order to be expected for $T > T_c$, a calculation of the elastic paramagnetic neutron-scattering cross section for normal cubic spinels with nearest-neighbor A-B and B-B exchange interactions is given, and contact is made with experiments on $MnCr_2O_4$.

I. INTRODUCTION

SERIES expansions of the thermodynamic functions in powers of $1/T$ have long served as standards by which to judge various approximation techniques, such as the molecular-field approximation, the Bethe-Peierls-Weiss cluster approximation, and the several Green's-function decoupling procedures.[1] Even for temperature as low as the critical temperature T_c, it is generally felt that the most reliable information is that obtained by extrapolation from the first few terms of high-temperature series expansions. Considerable effort along these lines has been directed toward using the high-temperature expansion of the zero-field susceptibility χ to estimate both the location of the critical singularity T_c,[2–4] and the form of the divergence of χ as $T \to T_c$ from above.[5–7] The first few terms of the corresponding high-temperature series for the zero-field magnetic specific heat C, entropy S, and internal energy U have also been computed.

The motivation for considering the spin correlation function $\langle \mathbf{S}_f \cdot \mathbf{S}_g \rangle_\beta$ rather than the customary quantities is that $\langle \mathbf{S}_f \cdot \mathbf{S}_g \rangle_\beta$ not only yields all of the thermodynamic functions,[8] but also provides information which is relevant to current experiments and is not obtainable from the thermodynamic functions:

(1) $\langle \mathbf{S}_f \cdot \mathbf{S}_g \rangle_\beta$ contains information concerning the location of the critical temperature T_c for substances which order to a spin configuration other than ferromagnetic.[9] Substantial improvement over previous estimates of T_c for normal cubic spinels possessing both A-B and B-B nearest-neighbor Heisenberg exchange interactions has been obtained as follows: Instead of defining T_c as the temperature at which ordinary susceptibility diverges, one defines T_c as the temperature at which the maximum "generalized Fourier amplitude" of $\langle \mathbf{S}_f \cdot \mathbf{S}_g \rangle_\beta$ diverges.[10] This generalized Fourier amplitude is just the usual Fourier amplitude, suitably generalized for lattices with more than one spin per unit cell. In the special case where ferromagnetism is expected, the divergent Fourier amplitude is essentially χ.

(2) $\langle \mathbf{S}_f \cdot \mathbf{S}_g \rangle_\beta$ contains information concerning the *type* of long-range magnetic ordering to be expected for $T \lesssim T_c$.[10] Previous applications of the high-temperature series to the study of critical phenomena have assumed the type of ordering to be given at the outset

---

* This work constitutes part of a Ph.D. thesis submitted to the Physics Department of Harvard University, January, 1967.

† Operated with support from the U.S. Air Force.

[1] See, e.g., W. Opechowski, Physica **4**, 181 (1937); **6**, 1112 (1938); J. H. Van Vleck, J. Chem. Phys. **5**, 320 (1937); B. Strieb, H. B. Callen, and G. Horwitz, Phys. Rev. **130**, 1798 (1963); H. B. Callen, *ibid.* **130**, 890 (1963).

[2] H. A. Brown and J. M. Luttinger, Phys. Rev. **100**, 685 (1955).

[3] G. S. Rushbrooke and P. J. Wood, Mol. Phys. **1**, 257 (1958).

[4] C. Domb and D. W. Wood, Proc. Phys. Soc. (London) **86**, 1 (1965).

[5] C. Domb and M. F. Sykes, Phys. Rev. **128**, 168 (1962).

[6] J. Gammel, W. Marshall, and L. Morgan, Proc. Roy. Soc. (London) **A275**, 257 (1963).

[7] G. A. Baker, H. E. Gilbert, J. Eve, and G. S. Rushbrooke, Phys. Rev. Letters **20**, 146 (1966).

[8] As an example of the applicability of the series expansion of $\langle \mathbf{S}_f \cdot \mathbf{S}_g \rangle_\beta$ to obtain the corresponding high-temperature series expansion of the zero-field magnetic susceptibility, see H. E. Stanley, following paper, Phys. Rev. **158**, 546 (1967).

[9] K. Dwight, T. A. Kaplan, H. E. Stanley, and N. Menyuk, M.I.T. Lincoln Laboratory Solid State Research Report No. 4, DDC 613961, 1964 (unpublished).

[10] T. A. Kaplan, H. E. Stanley, K. Dwight, and N. Menyuk, J. Appl. Phys. **36**, 1129 (1965).

and, furthermore, have been restricted to only two types of ordering—ferromagnetic and antiferromagnetic.[1–7] Thus this previous work is not applicable to the class of substances which order at $T=T_c$ to a spiral spin configuration. A method has recently been suggested[10] for determining the type of magnetic ordering to be expected for a given model Hamiltonian, based not on the divergence to ∞ of χ but rather on the essential physical fact that as the ordering temperature is approached from above, the spin correlation function $\langle \mathbf{S}_f \cdot \mathbf{S}_g \rangle_\beta$ becomes long range. The preliminary results suggest that this new approach will give reasonably definitive answers to the question of the type of ordering.[11]

(3) $\langle \mathbf{S}_f \cdot \mathbf{S}_g \rangle_\beta$ contains the information about the short-range magnetic order for $T > T_c$ needed to compute the diffuse paramagnetic neutron-scattering cross section.[12] The utility of the *time-dependent* spin-spin correlation function $\langle \mathbf{S}_f(t) \cdot \mathbf{S}_g(0) \rangle_\beta$ has for several years been recognized, particularly because of the fact that its Fourier transform in space and time is proportional to the inelastic neutron-scattering cross section. Saenz has argued that for thermal neutrons of wavelength ~ 1Å and all but the smallest scattering angles, one may restrict oneself to a calculation of the *time-independent* (static) correlation function $\langle \mathbf{S}_f \cdot \mathbf{S}_g \rangle_\beta$.[13] The elastic paramagnetic neutron-scattering cross section was recently calculated from the high-temperature expansion of $\langle \mathbf{S}_f \cdot \mathbf{S}_g \rangle_\beta$ for a Heisenberg-model Hamiltonian, and reasonable quantitative agreement with the experimental results for several chromium spinels was obtained for temperatures well above T_c.[12]

In the following section we shall describe a high-temperature series expansion for the zero-field static spin correlation function which is valid both quantum mechanically and classically. In Sec. III, the simplifications of the classical Heisenberg model are exploited to obtain the diagrammatic representation of the first nine coefficients in the expansion for loose-packed lattices and the first eight coefficients for close-packed lattices. As an example of the applicability of the series expansion of $\langle \mathbf{S}_f \cdot \mathbf{S}_g \rangle_\beta$ to provide information concerning the short-range magnetic order to be expected for $T > T_c$, a calculation of the elastic paramagnetic neutron cross section for a normal cubic spinel with nearest-neighbor A-B and B-B exchange interactions is presented in Sec. IV. The cross section for successive truncations of the series expansion is plotted as a function of scattering angle for $MnCr_2O_4$, and contact is made with recent experimental results.

[11] The results indicate that correlation corrections to the predictions of the molecular-field approximation (which corresponds to calculating only the first term of the high-temperature series expansion) can have significant effects on the type of long-range magnetic ordering.

[12] K. Dwight, N. Menyuk, and T. A. Kaplan, J. Appl. Phys. **36**, 1090 (1965).

[13] A. W. Saenz, Phys. Rev. **119**, 1542 (1960).

II. SERIES EXPANSION OF THE SPIN CORRELATION FUNCTION

Recently Stanley and Kaplan[14] (SK) have discussed a high-temperature series expansion

$$\frac{\text{trace } \mathbf{S}_f \cdot \mathbf{S}_g e^{-\beta \mathcal{H}}}{\text{trace } e^{-\beta \mathcal{H}}} = \sum_{l=0}^{\infty} \frac{(-1)^l}{l!} \alpha_l \beta^l \tag{1}$$

of the zero-field static spin correlation function $\langle \mathbf{S}_f \cdot \mathbf{S}_g \rangle_\beta$ between spins $\mathbf{S}_f$ and $\mathbf{S}_g$ localized on the sites f and g. Here $\beta = 1/kT$ and $\mathcal{H}$ is the spin Hamiltonian in zero magnetic field.

The coefficients α_l occurring in Eq. (1) satisfy the recursion relation

$$\alpha_l = \nu_l - \sum_{k=0}^{l-1} \binom{l}{k} \alpha_k \mu_{l-k}, \tag{2}$$

where $\nu_l \equiv \langle \mathbf{S}_f \cdot \mathbf{S}_g \mathcal{H}^l \rangle$, $\mu_m \equiv \langle \mathcal{H}^m \rangle$, and $\langle \mathcal{O} \rangle \equiv \text{trace } \mathcal{O}/\text{trace } 1$ denotes the $\beta = 0$ thermal average of the operator $\mathcal{O}$. Rushbrooke and Wood (RW)[3] have explained in detail a diagrammatic representation of the moments $\mu_m = \sum_d \mu_m(d)$, and SK have outlined a diagrammatic representation of the coefficients α_l and ν_l. Since $\mathcal{H} = \sum_{ij} J_{ij} \mathbf{S}_i \cdot \mathbf{S}_j \equiv \sum_{ij} \mathcal{O}_{ij}$, $\nu_l = \langle \mathbf{S}_f \cdot \mathbf{S}_g \mathcal{H}^l \rangle$ is a sum of averages $\langle \mathbf{S}_f \cdot \mathbf{S}_g \prod O_{ij} \rangle$ of a product of l factors O_{ij} and one factor $\mathbf{S}_f \cdot \mathbf{S}_g$. For each of the l factors O_{ij} in the product, SK draw a straight line connecting sites i and j; for the factor $\mathbf{S}_f \cdot \mathbf{S}_g$, a wavy "correlation" line connects the given fixed sites f and g. The collection of these $(l+1)$ lines corresponding to the entire product is the diagram $\bar{d}$ associated with that product. Thus $\nu_l = \sum_{\bar{d}} \nu_l(\bar{d})$, and we have obtained a diagrammatic representation of $\alpha_l = \sum_{\bar{d}} \alpha_l(\bar{d})$, with

$$\alpha_l(\bar{d}) = \nu_l(\bar{d}) - \sum_{k=0}^{l-1} \sum_{\bar{d}_a, d_b}{}' \alpha_k(\bar{d}_a) \mu_{l-k}(d_b), \tag{3}$$

as may be proved from Eq. (2) by induction. The restricted summation $\sum'$ is over all partitions of $\bar{d}$ into diagrams $\bar{d}_a$, d_b such that the sum $\bar{d}_a + d_b = \bar{d}$. Equations (2) and (3) are valid quantum mechanically as well as classically.

III. CLASSICAL CALCULATION

Although the development of the preceding section is valid for the quantum-mechanical Heisenberg model, the order-of-magnitude simplifications which occur in any explicit calculation when one treats the noncommuting quantum-mechanical spin operators occurring in the Heisenberg Hamiltonian $\mathcal{H} = -\sum_{ij} J_{ij} \mathbf{S}_i \cdot \mathbf{S}_j$ as commuting vectors of length $\bar{S}$, where $\bar{S}^2 \equiv S(S+1)$, suggest that many more terms in the series can be obtained "classically" than "quantum mechanically." Moreover, SK argued that *useful* results in the critical region ($T \cong T_c$) could be obtained from this classical Heisenberg model or "infinite-spin approximation," the

[14] H. E. Stanley and T. A. Kaplan, Phys. Rev. Letters **16**, 981 (1966).

errors in various critical properties of interest being small and decreasing rapidly with S—for example, the errors in the extrapolated estimates of $T_c/\bar{S}$ for cubic lattices are only $\sim 4\%$ for $S=1$ and $\sim 1\%$ for $S=5/2$.[15]

The utility of the diagrammatic representation described above is that $\alpha_l(\bar{d})$ depends only upon the topology of the diagram $\bar{d}$, and not upon the angles between the lines. Thus for a given order l one need calculate only the different $\alpha_l(\tau)$, where τ indexes the "topological type" of diagram $\bar{d}$. Although there are many different topological types of diagrams with l straight lines and one wavy line which might potentially contribute to α_l, SK showed that $\alpha_l(\tau)$ is zero for a large majority of these types. The only "classical diagrams" or diagrams which *do* contribute to the classical calculation were found to be those which are at the same time both stars[16] and continuous paths.[17] Thus one can ignore all diagrams which contain one or more articulation points (trees), all disconnected diagrams,[18] and all diagrams which contain one or more "odd vertices" (vertices at which an odd number of lines meet).

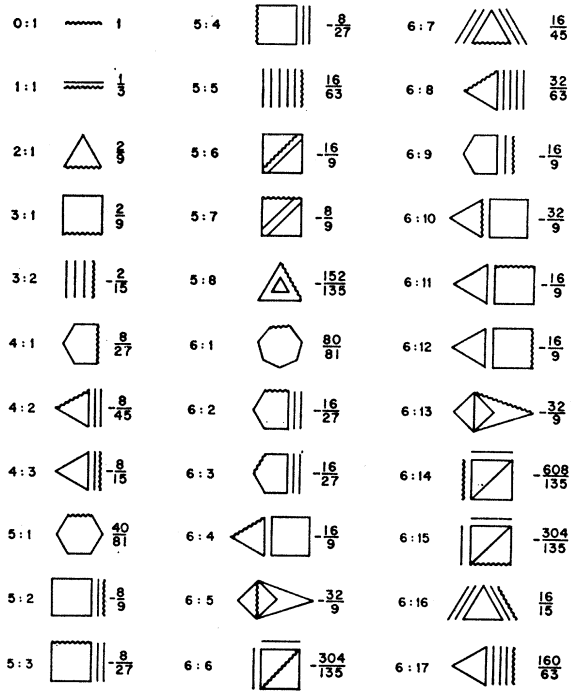

FIG. 1. The diagrams $(l{:}\tau)$ contributing to the high-temperature series expansion for $\langle \mathbf{S}_f \cdot \mathbf{S}_g \rangle_\beta$ through order $l=6$ and their corresponding $[\alpha_l(\tau)]$.

Thus to find α_l classically we must (i) enumerate all classical diagrams of l straight lines and one wavy correlation line; (ii) calculate the average $\nu_l(\bar{d})$; (iii) use the recursion relation in Eq. (3) to get $\alpha_l(\bar{d})$.

Step (i) requires finding all continuous paths which are free of articulation points, and the results through order $l=8$ are shown in Figs. 1–4. Figure 5 includes the order $l=9$ diagrams required for loose-packed lattices. We have represented each diagram by the notation $(l{:}\tau)$, where l is the number of straight lines and τ indexes the topological type of diagram. We notice that the number of diagrams required for a given order l increases very rapidly with l; for $l=1, 2, \cdots, 8$, there are 1, 1, 2, 3, 8, 17, 47, 123 classical "correlation function diagrams" of l straight lines and one wavy line. These numbers are roughly an order of magnitude smaller than the corresponding numbers of quantum-mechanical correlation function diagrams. Moreover, if we restrict the range of the exchange interaction to nearest neighbors only, and also exclude the close-packed (e.g., plane triangular and face-centered cubic) lattices, we need consider only 1, 1, 2, 2, 5, 8, 20, 35 classical diagrams.[19]

The enormous labor required to perform step (ii) when the spin operators do not commute is the primary

[15] The errors in the extrapolated estimates of $T_c/\bar{S}^2$ for the common *two-dimensional* lattices are much larger, since here $T_c^{(2)}/\bar{S}^2 \sim 2-1/\bar{S}^2$. [See H. E. Stanley and T. A. Kaplan, Phys. Rev. Letters **17**, 913 (1966); J. Appl. Phys. **38**, 975 (1967); H. E. Stanley (unpublished).] To be sure, the errors in quantities pertaining to other temperature domains may not be small: e.g., the ground-state energy is proportional to $S(S+1)$ classically, to S^2 quantum mechanically.

[16] By standard definition, a "star" is a connected graph which contains no articulation points. An articulation point has the property that if all the lines to it are cut the graph becomes disconnected; that is, it becomes possible to separate the points of the graph in two or more groups such that there is no line joining a point of one group with a point of the other. Excluding nonstar graphs is thus equivalent to excluding disconnected graphs and tree graphs. See, e.g., G. E. Uhlenbeck and G. W. Ford, in *Studies in Statistical Mechanics*, edited by J. DeBoer and G. E. Uhlenbeck (North-Holland Publishing Company, Amsterdam, 1962), p. 125.

[17] A continuous path is one which can be entirely traced out (using every straight line once and only once) from vertex f to vertex g without lifting one's pencil from the paper. This implies that a noncontinuous path has at least one "odd vertex"—i.e., a vertex at which an odd number of lines meet. The odd vertex will contribute an odd number of spin vectors to the integrand of $\nu_l(\bar{d})$, so that $\nu_l(\bar{d})=0$. Similarly, $\mu_l(d)=0$ for d noncontinuous, so that from Eq. (3) it is easy to see that $\alpha_l(\bar{d})=0$.

[18] Our method of calculating χ directly from the SK diagrammatic representation of the spin correlation function (Ref. 8) is simpler than using the RW moment expansion to calculate χ, largely because the two sizeable classes of disconnected diagrams and, classically, diagrams with articulation points contribute to their moment expansion and not to our Eq. (3). Our method is also less susceptible to careless errors than the RW moment method because one can partition diagrams into their subdiagrams [as required for Eq. (3) of the SK method] more easily than one can determine all possible ways of putting subdiagrams together into larger diagrams (as required to count the number of occurrences for the RW disconnected diagrams). (See Appendix A.) Recently Wood and Rushbrooke [Phys. Rev.Letters **17**, 307 (1966)] have obtained—for the fcc, bcc, and sc lattices—eight terms in the susceptibility series for the classical Heisenberg model using the RW moment expansion. Our calculation of the susceptibility for general lattices (presented in Ref. 8) agrees term by term with Wood and Rushbrooke when we specialize to the class of three-dimensional cubic lattices they considered.

[19] This very marked reduction arises from the well-known fact that for the loose-packed lattices one can ignore all diagrams containing polygons with an odd number of straight lines. For example, triangles can be ignored since it is impossible to find three sites in the loose-packed lattices such that all three are nearest neighbors of one another.

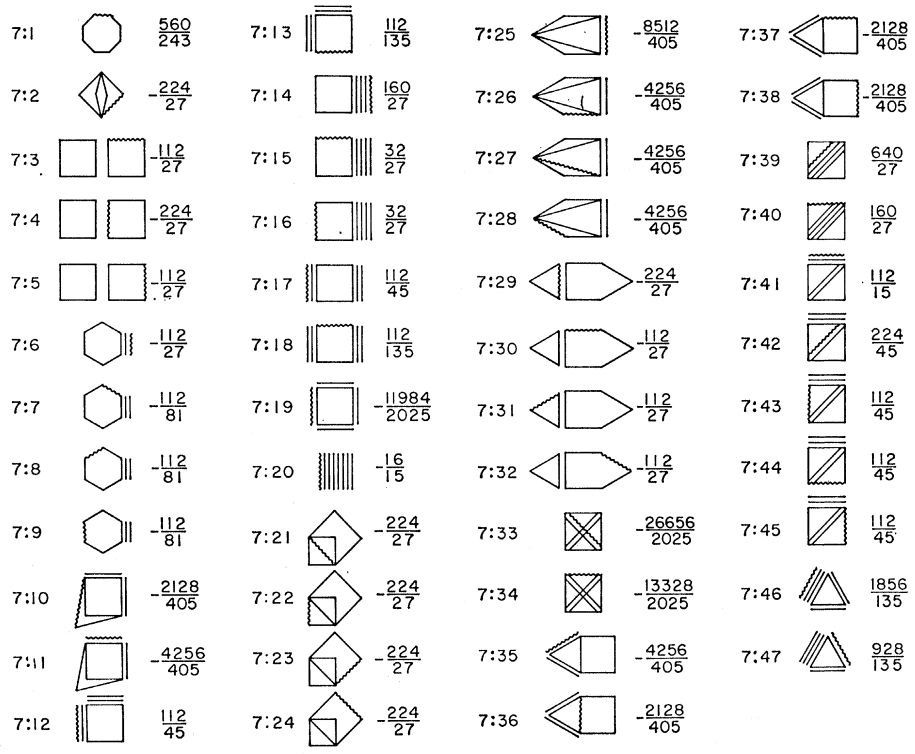

FIG. 2. The 47 different topological types $(7{:}\tau)$ of diagrams required to extend the high-temperature expansion to order $l=7$ and the corresponding $[\alpha_7(\tau)]$. Only the first 20 diagrams $(\tau=1-20)$ contribute for loose-packed lattices with nearest-neighbor interactions.

reason any extension of the quantum-mechanical high-temperature expansion is impractical.[3] However, for the classical calculation the averages required for (ii) are simple (in fact, there exists no single limiting factor prohibiting the extension of the classical series). Moreover, a theorem similar to Theorem IV of RW was found to be very helpful because it allows one to express $\nu_l(\bar{d})$ in terms of corresponding $\mu_{l+1}(d)$:

Theorem A. If d is the RW moment diagram obtained from $\bar{d}$ by replacing the wavy correlation line in $\bar{d}$ by a straight line, then

$$[\nu_l(\bar{d})]=\frac{P(\bar{d})}{P(d)}[\mu_{l+1}(d)], \tag{4}$$

where $P(\bar{d})$ and $P(d)$ are, respectively, the number of permutations of the straight lines in $\bar{d}$ and d, and the bracketed quantities $[\nu]$ and $[\mu]$ denote ν and μ with all factors $-2J_{ij}$ and $S_i(S_i+1)$ omitted. RW have described in detail a straightforward method of obtaining the requisite moments $\mu_{l+1}(d)$.[3] Especially useful is their Theorem I, which simplifies still further the calculation of a trace for the more "open" diagrams (e.g., an eight-sided polygon) by relating it to the trace of a lower-order diagram.

Step (iii), applying the recursion relation in Eq. (3) to get $\alpha_l(\bar{d})$, is not difficult. All that is required is to partition the diagram $\bar{d}$ into all subdiagrams $\bar{d}_a$ and d_b such that their sum $\bar{d}_a+d_b=\bar{d}$, since the calculation of

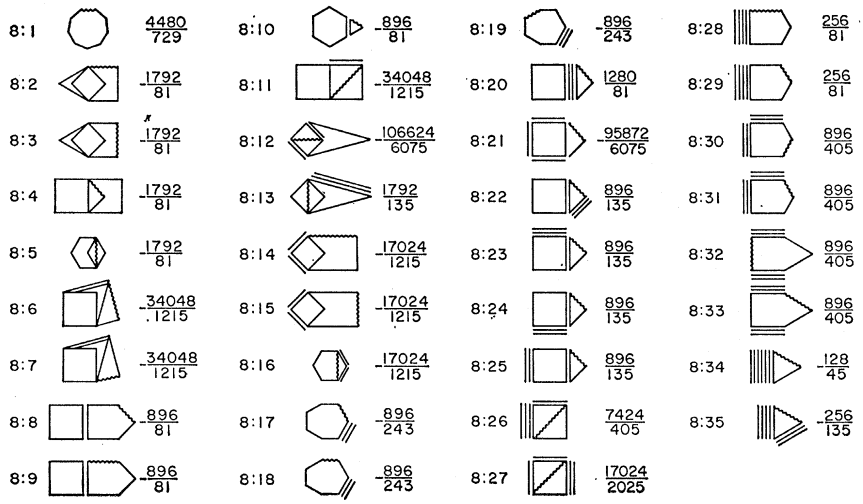

FIG. 3. The 35 diagrams $(8{:}\tau)$ and the corresponding $[\alpha_8(\tau)]$ which are needed to extend the high-temperature series to order $l=8$ for the restricted class of loose-packed lattices with interactions only between nearest neighbors.

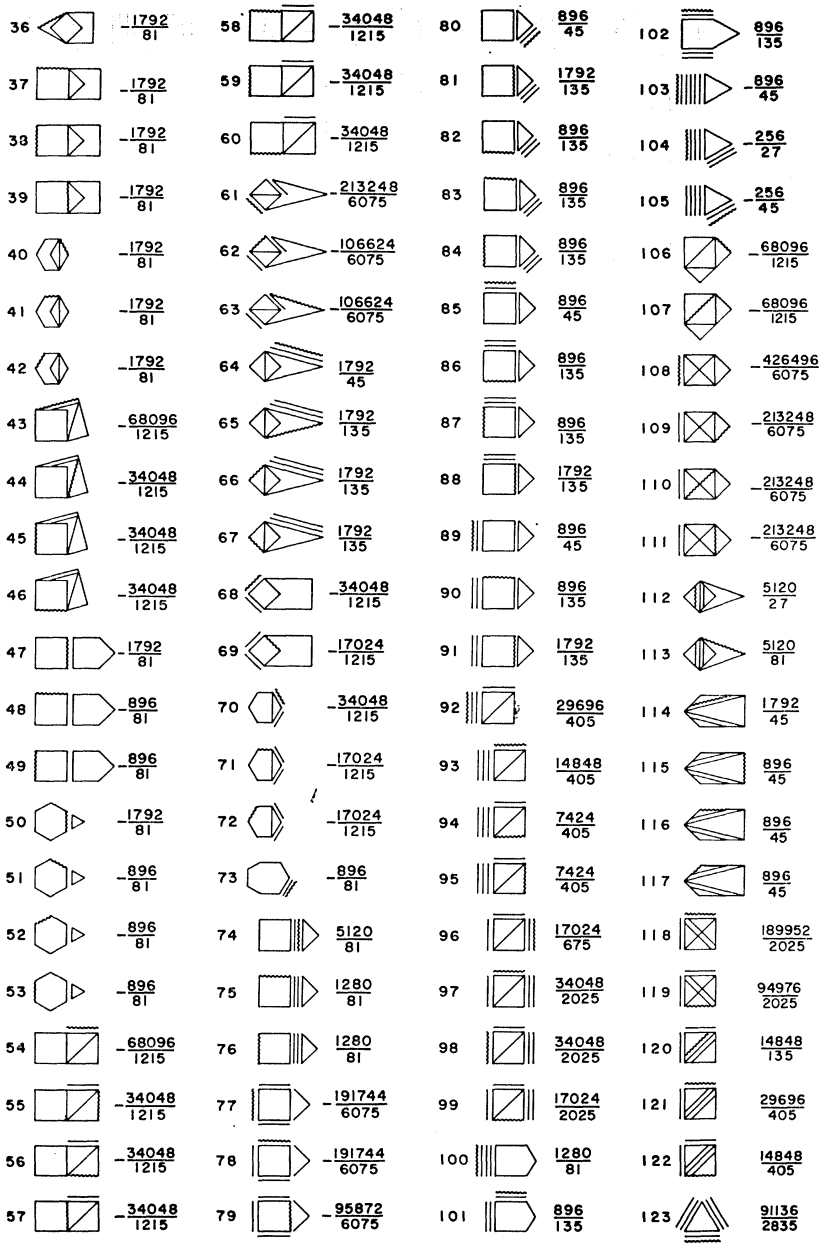

FIG. 4. The 88 additional diagrams (8:τ) needed for order $l=8$ if close-packed (e.g., plane triangular and face-centered cubic) lattices are to be included.

the requisite $\alpha_k(\bar{d}_a)$ and $\mu_{l-k}(d_b)$ will already have been carried out in the course of obtaining $\alpha_{l'}$, $l'<l$.[20] Use of the recursion relation would not be necessary if one were to choose a different diagrammatic representation of the spin correlation function (one closely akin to the RW moment expansion), but then one would be required to count the number of occurrences of disconnected diagrams and diagrams with articulation points—a cumbersome procedure.

As an illustrative example, we carry out the calculation of the contribution to α_4 arising from the diagram $\bar{d}$ in Fig. 1 of topological type (4:3). In part (a) of Fig. 6, Theorem A is used to relate $[\nu_4(\bar{d})]$ to the corresponding $[\mu_5(d)]$, where $P(\bar{d})=4!/2!$ and $P(d)=5!/3!$. To facilitate the evaluation of the moment $[\mu_5(d)]$, we observe that since the integral over all spins except one, say S_f, is independent of the orientation of S_f, we can choose a z axis to be along $\mathbf{S}_f$; i.e., $\mathbf{S}_f=(0, 0, S_f)$. Then the integrand $(\mathbf{S}_f\cdot\mathbf{S}_g)^3\mathbf{S}_f\cdot$

[20] To be sure, the moments $\mu_{l-k}(d_b)$ corresponding to a partitioning $\bar{d}=\bar{d}_a+d_b$ such that d_b is either disconnected or contains an articulation point *will* contribute to the recursion relation in Eq. (3). Although such moments $\mu_{l-k}(d_b)$ will *not* yet have been obtained [in the course of using Theorem A to obtain $\alpha_{l-k}(\bar{d})$], their evaluation is very simple: If a diagram d (with m straight lines) may be partitioned into subdiagrams d_1, d_2 (with m_1, m_2 lines, respectively) which are either disconnected or else have only one point in common (an articulation point), then $\mu_m(d)=(m!/m_1!m_2!)\mu_{m_1}(d_1)\mu_{m_2}(d_2)$.

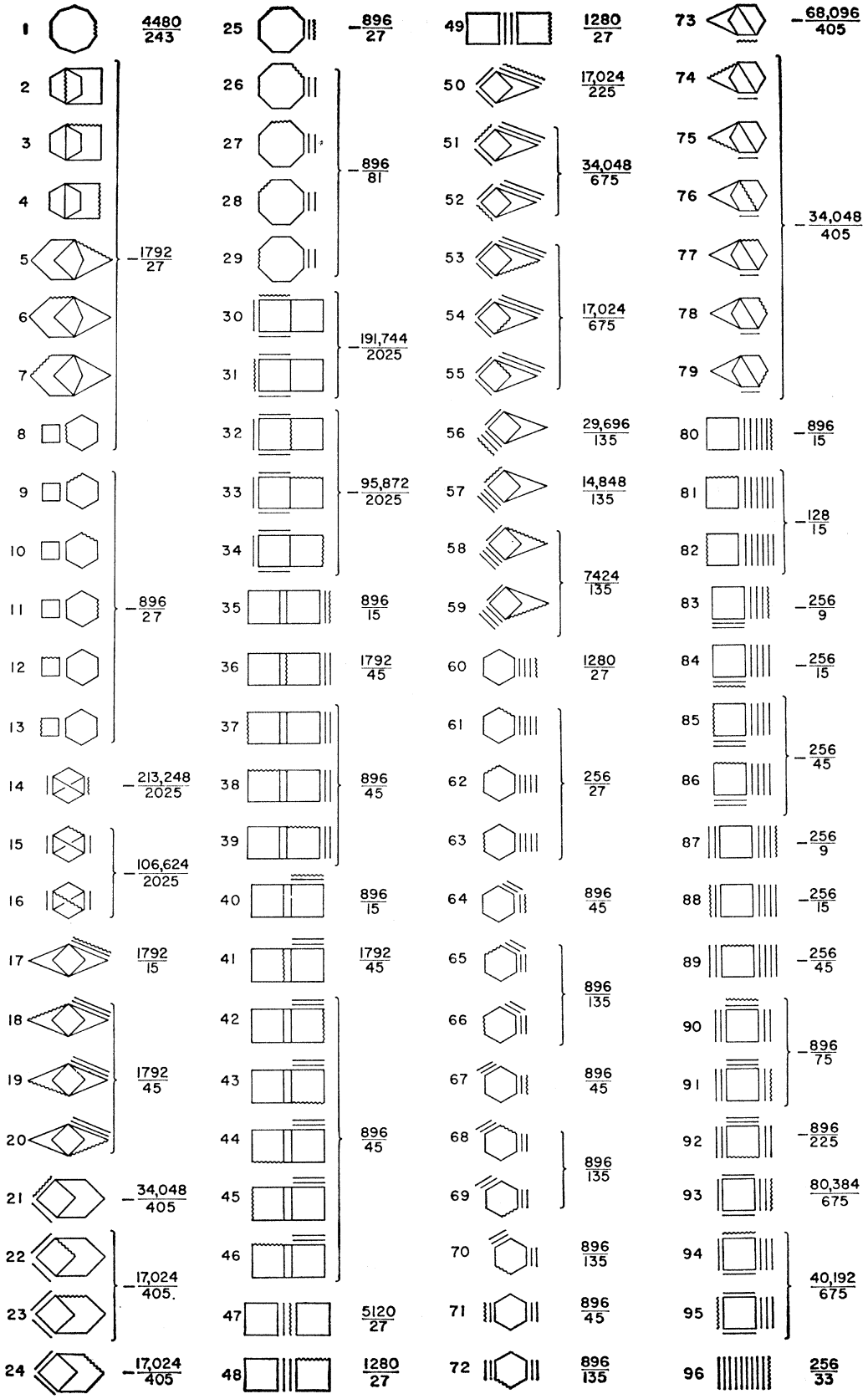

FIG. 5. The 96 diagrams $(9:\tau)$ required for loose-packed lattices in ninth order.

$\mathbf{S}_p\mathbf{S}_g\cdot\mathbf{S}_p$ becomes simply

$$\sum_{j=x,y,z} S_{fz}{}^4 S_{gz}{}^3 S_{gj} S_{pz} S_{pj},$$

and the integral factors into the "single-spin averages" shown on the second line of Fig. 6(a). These vanish whenever a spin is raised to an odd power (e.g., if $j=x$ or y, $\langle S_z S_j\rangle=0$). If all the spins are raised to even powers, then the single-spin averages may be evaluated in closed form:

$$\langle S_x{}^{2k} S_y{}^{2l} S_z{}^{2m}\rangle = (2\pi)^{-1}\frac{\Gamma(k+\frac{1}{2})\Gamma(l+\frac{1}{2})\Gamma(m+\frac{1}{2})}{\Gamma(k+l+m+\frac{3}{2})}. \quad (5)$$

Part (b) of Fig. 6 illustrates step (iii)—how to use the recursion relation to finally obtain the contribution to α_4 from diagram (4:3). All partitions of diagram (4:3) besides the two shown in part (b) of Fig. 6 are such that $\alpha_k(\bar{d}_a)$ and $\mu_{l-k}(d_b)$ are both zero.

In this fashion we calculated all of the $\alpha_l(\tau)$ required for any lattice through order $l=8$, and the results of this calculation are given in Figs. 1–4. Figure 5 represents an extension to order $l=9$ for the loose-packed lattices only. For nearest-neighbor (n.n.) interactions and equivalent spins, the numbers $[\alpha_l(\tau)]$ given to the right of each diagram are in fact just the $\alpha_l(\tau)$ without any of the factors $(-2J)$ and $\bar{S}^2=S(S+1)$; the $\alpha_l(\tau)$ can be obtained from the relation

$$\alpha_l(\tau)=\bar{S}^2(-2J\bar{S}^2)^l[\alpha_l(\tau)]. \quad (6)$$

For other than n.n. interactions, we need to carry along the factors J_{ij}; for inequivalent spins we need to distinguish $\bar{S}_i{}^2\equiv S_i(S_i+1)$ and $\bar{S}_j{}^2\equiv S_j(S_j+1)$.[21] The

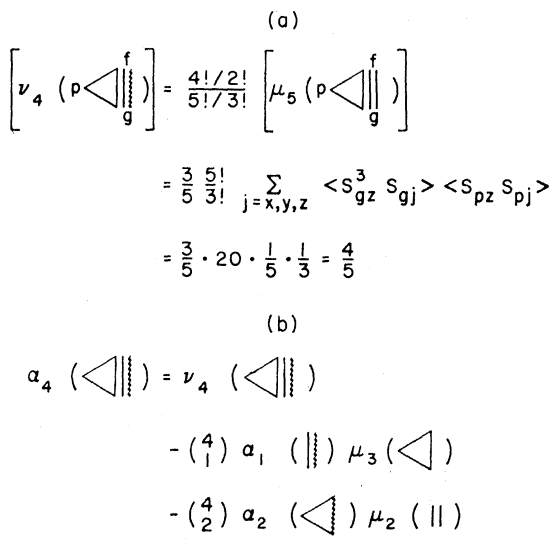

FIG. 6. (a) Application of Theorem A to obtain $[\nu_4(\bar{d})]$ for the diagram $\bar{d}=(4{:}3)$ (see Fig. 1) from the corresponding moment $[\mu_5(d)]$. (b) Application of the recursion relation Eq. (3), to obtain the contribution to α_4 from diagram (4:3).

[21] Inequivalent spins (a different magnetic moment on different sites) can be allowed for by renormalizing all spin vectors to unit vectors and all exchange integrals J_{ij} to $\bar{J}_{ij}=\bar{S}_i\bar{S}_jJ_{ij}$.

numerical values of the $[\alpha_l(\tau)]$ in Figs. 1–5 are unaffected, but Eq. (6) is no longer valid. The $\alpha_l(\tau)$ can nevertheless be obtained from the $[\alpha_l(\tau)]$ almost by inspection. For example, if we wish to calculate the high-temperature series expansion for a normal cubic spinel lattice with Heisenberg exchange interactions J_{B-B} between n.n. B-site cations, and J_{A-B} between A- and B-site cations which are nearest neighbors, we need to distinguish different magnitudes of the exchange interactions, J_{B-B} and J_{A-B}, and also different magnitudes S_A and S_B of the spin magnetic moments on the A and B sites. Thus, $\alpha_1(1)=\bar{S}_f{}^2J_{fg}$, $\alpha_2(1)=-2J_{fg}\bar{S}_f{}^2\bar{S}_g{}^2/3$, etc., where f, g may be either A or B sites.

IV. EXAMPLE: PARAMAGNETIC NEUTRON SCATTERING

Normal Cubic Spinel with Nearest-Neighbor A-B and B-B Interactions

We now apply the diagrammatic representation of the classical coefficients α_l to obtain to order $l=4$ the high-temperature expansion of the paramagnetic neutron-scattering cross section for a normal cubic spinel lattice with Heisenberg exchange interactions J_{B-B} between n.n. B-site cations, and J_{A-B} between n.n. A- and B-site cations. For a powder sample above the critical temperature, $\mathfrak{F}_M(2\theta)\propto F_M{}^2(q)\mathfrak{F}_0$, where $\mathfrak{F}_0$ and $\mathfrak{F}_M$ are the incident and magnetically scattered neutron fluxes, 2θ is the scattering angle (related to q via $4\pi\sin\theta=\lambda q$), and

$$F_M{}^2(q)=\sum_{\nu,m\mu} f_\nu f_\mu g_\nu g_\mu \langle \mathbf{S}_{n\nu}\cdot\mathbf{S}_{m\mu}\rangle_\beta j_0(q\tau_{n\nu}{}^{m\mu}). \quad (7)$$

Here $j_0(x)\equiv(\sin x)/x$, g_ν is the g factor, $f_\nu(q)$ is the form factor, $\boldsymbol{\tau}_{n\nu}{}^{m\mu}\equiv\mathbf{R}_{n\nu}-\mathbf{R}_{m\mu}$ is the site-separation vector, and $R_{n\nu}$ denotes a vector to the νth site in the nth unit cell.

To obtain a high-temperature series expansion of the function $F_M{}^2(q)$ in Eq. (7) from the diagrammatic representation of the corresponding high-temperature series expansion of the spin correlation function $\langle\mathbf{S}_{n\nu}\cdot\mathbf{S}_{m\mu}\rangle_\beta$, we must sum the contribution $\alpha_l(\tau)$ of each different topological type of diagram over all sites $n\nu$ and $m\mu$. This procedure is very lengthy and is certainly the limiting factor in how far one can carry the expansion. Dweight *et al.*[12] published the quantum-mechanical calculation to order $l=3$; in Appendix B we express $F_M{}^2(q)$ for a spinel with n.n. A-B and B-B interactions through order $l=4$ within the classical Heisenberg model.

Manganese Chromite

Hastings and Corliss[22] have studied the behavior of the broad liquid-type peak in the cubic spinel $MnCr_2O_4$, and found that it persisted at temperatures as high as several times the critical temperature. Recently, Dwight *et al.*[12] were able to obtain agreement with the room-

[22] J. M. Hastings and L. M. Corliss, Phys. Rev. **126**, 556 (1962).

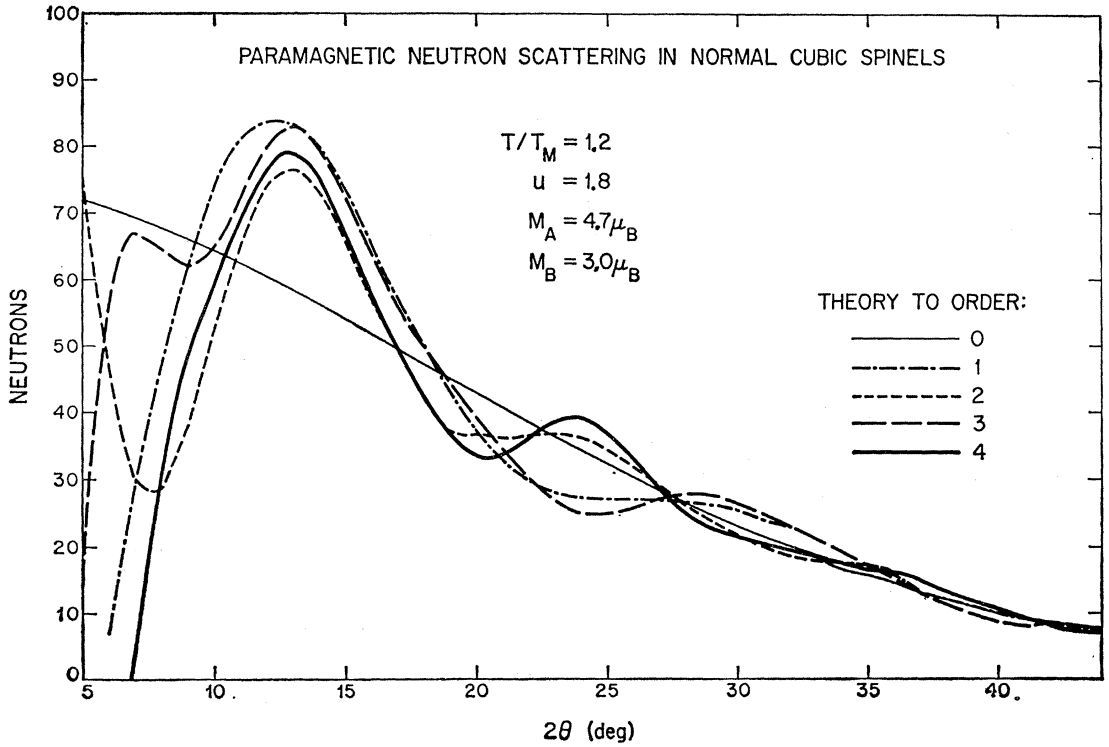

FIG. 7. Successive truncations at orders $l=0, 1, \cdots, 4$ of the high-temperature expansion of Eq. (7) for the paramagnetic elastic neutron scattering cross section at a temperature $T=1.2\ T_M \cong 100°K$. To specialize to $MnCr_2O_4$, we have chosen $u \equiv 4J_{BB}S_B/3J_{AB}S_A$ to have the value 1.8, S_A and S_B to be 5 and 3, respectively, and the magnetic moments on the A and B sites to be 4.7 and 3.0 μ_B, respectively (i.e., the g factor on the A sites is 1.87, not 2).

temperature ($T=300°K \cong 7T_c$) pattern of Hastings and Corliss from a truncation of the high-temperature expansion Eq. (1) at order $l=1$. At lower temperatures, however, the convergence of the terms of the order $l=3$ quantum-mechanical calculation is poor. We find that, through order $l=3$, the predictions of the classical Heisenberg model differ only slightly from those of the quantum-mechanical Heisenberg model. Consequently, there is some reason to believe that an extension of the series to higher order for the classical Heisenberg model will give meaningful results for $MnCr_2O_4$.

In Fig. 7 we plot the successive truncations $l=0, 1, \cdots, 4$ of the high-temperature expansion of the paramagnetic neutron-scattering cross section against scattering angle 2θ for $MnCr_2O_4$ *at a temperature only one-third of room temperature.* We see that the truncations at orders 1, 2, and 3 do not seem to be converging for the amplitude of the peak at $2\theta \cong 13°$. Addition of the fourth-order term serves to suggest that the limiting value of the amplitude may lie somewhere in between 75 and 80—an accuracy of $\sim 7\%$. On the other hand, convergence of the first four truncations at $2\theta \cong 25°$ is poor, suggesting the calculation of more terms may be useful.

V. SUMMARY

We have taken advantage of the simplifications which result if one treats the spin operators as classical vectors of length $\bar{S}$ to obtain the diagrammatic representation of the first nine coefficients α_l for loose-packed lattices and the first eight α_l for close-packed lattices in the high-temperature expansion [Eq. (1)] of the zero-field spin correlation function $\langle \mathbf{S}_f \cdot \mathbf{S}_g \rangle_\beta$. The utility of the series expansion of $\langle \mathbf{S}_f \cdot \mathbf{S}_g \rangle_\beta$ was illustrated by a calculation of the elastic paramagnetic neutron cross section and contact was made with experimental measurements[22] on $MnCr_2O_4$. The present calculation is applied elsewhere[8] to obtain the corresponding high-temperature series expansion of the zero-field susceptibility χ.

ACKNOWLEDGMENTS

I am greatly indebted to Dr. Thomas A. Kaplan for many stimulating discussions, for much valuable advice, and for assistance in preparing this manuscript. Thanks are also due Kirby Dwight for his help, encouragement, and friendly advice; his assistance was essential in carrying out the neutron-scattering calculation described in Sec. IV. I am grateful to Professor J. H. Van Vleck and Dr. Herbert J. Zeiger for their interest and support throughout the course of this research.

APPENDIX A: RELATION TO RUSHBROOKE-WOOD MOMENT EXPANSION

There are essentially two differences between the method used here and the moment expansion of the

partition function $Z \equiv \mathrm{Tr}\, e^{-\beta \mathcal{H}}$ used by RW[3]:

(1) We utilize a recursion relation, which leads to a marked reduction in the number of diagrams.

(2) We focus on the spin correlation function.

(1) Wood and Rushbrooke were required (by their moment-expansion method) to count the number of occurrences of two sizeable classes of diagrams—disconnected diagrams and diagrams containing articulation points (trees).[3,18] We were required to count only about half as many diagrams (only the star diagrams), the counting problem associated with the trees and disconnected diagrams having been taken into account by our use of the recursion relation in Eq. (3). In a sense the disconnected diagrams are "considered" when we *partition* the connected diagrams as required by the recursion relation. Clearly we never need even "consider" the trees; moreover, the process of partitioning the connected diagrams is simpler than that of counting the number of occurrences of disconnected diagrams. The possibility of using a recursion relation to obviate the need to count sizeable classes of diagrams does *not* require that one obtain χ from the spin correlation function—we have also proved such a recursion relation for the cumulants λ_l in the high-temperature expansion

$$\ln Z \propto \sum_{l=0}^{\infty} \lambda_l \beta^l.$$

Thus, if one wishes to calculate only the susceptibility, the relative *simplicity* of our work compared to the RW moment expansion arises solely from our use of a recursion relation.

(2) Consideration of the spin correlation function was motivated not as a more efficient method for obtaining $\chi (\propto \sum_R \langle \mathbf{S}_0 \cdot \mathbf{S}_R \rangle_\beta)$ but because there is much more information, relevant to recent experiments, contained in $\langle \mathbf{S}_f \cdot \mathbf{S}_g \rangle_\beta$ than in χ. (See discussion in Sec. I.) We have found that the diagrammatic representation for $\langle \mathbf{S}_f \cdot \mathbf{S}_g \rangle_\beta$ is the *same* as that required for χ alone; we have felt that it is sensible to record this diagrammatic representation because of the additional information contained therein, e.g., information concerning the short-range magnetic order to be expected for $T > T_c$ (as measured by the elastic paramagnetic neutron-scattering cross section), information concerning the *type* of long-range magnetic ordering to be expected for $T \lesssim T_c$ (as measured by neutron diffraction), and information concerning the location of T_c for substances which order to a spiral spin configuration.

APPENDIX B: HIGH-TEMPERATURE EXPANSION OF THE PARAMAGNETIC NEUTRON-SCATTERING CROSS SECTION

Here we obtain through order $l=4$ the high-temperature expansion

$$F_M^2(q) \equiv \sum_{l=0}^{\infty} \zeta_l x^l$$

of the paramagnetic neutron-scattering function in Eq. (7) for a general cubic spinel lattice with nearest-neighbor A-B and B-B interactions. Here $x \equiv J_{AB}\bar{S}_A\bar{S}_B/kT$, and the ζ_l are the coefficients to be evaluated. To simplify the expressions for the ζ_l, we define $A \equiv g_A f_A \bar{S}_A$, $B \equiv g_B f_B \bar{S}_B$, $U \equiv J_{BB}\bar{S}_B / J_{AB}\bar{S}_A$, and $\xi_n \equiv j_0(qa\sqrt{n})$; $a \equiv a_0/8$ denotes $\frac{1}{8}$ the cubic cell edge.

$$\zeta_0 = 2A^2 + 4B^2,$$

$$\zeta_1 = -16(UB^2\xi_8 + 2AB\xi_{11}),$$

$$\zeta_2 = (32/3)[(2U^2+3)B^2\xi_8 + 6UAB\xi_{11} + 2A^2\xi_{12} + (2U^2+4)B^2\xi_{24} + 6UAB\xi_{27} + (2A^2+U^2B^2+2B^2)\xi_{32} + 2B^2\xi_{40} + A^2\xi_{44}],$$

$$\begin{aligned}\zeta_3 = (-64/9)[&(20+1.4U^2)UB^2\xi_8 + (22.8+20U^2)AB\xi_{11} + 8UA^2\xi_{12} + 8(U^2+4)UB^2\xi_{24} + (30+22U^2)AB\xi_{27} \\ &+ (13A^2+26B^2+6U^2B^2)U\xi_{32} + (2U^2+20)UB^2\xi_{40} + 10UA^2\xi_{44} + 4(U^2+5)AB\xi_{43} + 4(U^2+5)UB^2\xi_{56} \\ &+ (14U^2+20)AB\xi_{59} + 2U(A^2+2B^2)\xi_{64} + (U^2+4)UB^2\xi_{72} + 12AB\xi_{75} + 4AB\xi_{91}],\end{aligned}$$

$$\begin{aligned}\zeta_4 = (16/27)[&(-48.5U^4+628.8U^2+403.2)B^2\xi_8 + (419.2U^2+1612.8)UAB\xi_{11} + (120U^2+86.4)A^2\xi_{12} \\ &+ (124.8U^4+1504U^2+649.6)B^2\xi_{24} + (483.2U^2+2323.2)UAB\xi_{27} + (448U^2+548.8)A^2\xi_{32} \\ &+ (150.4U^4+1296U^2+644.8)B^2\xi_{32} + 4(32U^4+260U^2+139.2)B^2\xi_{40} + (360U^2+438.4)A^2\xi_{44} \\ &+ 8(32U^2+176)UAB\xi_{43} + 32(7U^4+45U^2+24)B^2\xi_{56} + 16(39U^2+168)UAB\xi_{59} + 32(3U^2+5)A^2\xi_{64} \\ &+ 16(U^4+18U^2+10)B^2\xi_{64} + 8(10U^4+83U^2+46)B^2\xi_{72} + 32(6U^2+39)UAB\xi_{75} + 32(2U^2+21)UAB\xi_{91} \\ &+ 64(U^2+4)A^2\xi_{76} + 16(U^4+10U^2+17)B^2\xi_{88} + 32(3U^2+8)A^2\xi_{96} + 32(U^4+9U^2+8)B^2\xi_{96} \\ &+ 32(U^4+9U^2+9)B^2\xi_{104} + 16(7U^2+24)UAB\xi_{107} + 8(7U^2+12)A^2\xi_{108} + 64(U^2+2)B^2\xi_{120} + 96UAB\xi_{123} \\ &+ 8(6A^2+U^4B^2+6B^2)\xi_{128} + 64B^2\xi_{136} + 32UAB\xi_{139} + 64A^2\xi_{140} + 16B^2\xi_{152} + 16(A^2+B^2)\xi_{160}].\end{aligned}$$